# Solvent Effect on the Self-Assembled Structure of an Amphiphilic Perylene Diimide Derivative

**Xin Yang, Xiaohe Xu, and Hai-Feng Ji***

*Department of Chemistry, Institute for Micromanufacturing, Louisiana Tech University, Ruston, Louisiana 71272*

*Received: February 17, 2008; Revised Manuscript Received: April 6, 2008*

An amphiphilic electron-deficient (n-type) perylene diimide has been synthesized and characterized. The diimide contains a hydrophobic long chain on one end and a hydrophilic ethoxy chain on the other. The self-assembly of this molecule in polar and nonpolar solvents has been demonstrated by concentration- and temperature-dependent absorption and fluorescence spectroscopies. Analysis of the spectral change for the aggregates shows typical J-aggregates for structures precipitated from polar solvents and H-aggregates for structures precipitated from nonpolar solvents. SEM and TEM micrographs and a suggested packing scheme, compatible with the formation of nanostrips in nonpolar solvents and nanofibers in polar solvents, are presented.

## Introduction

Self-assembly of organic molecules in solutions is a fundamental step in designing bottom-up electronic and optoelectronic devices. Recent breakthroughs in organic memories[1] and IBM's first-ever use of self-assembly as part of microchip fabrication have validated the concept and feasibility of the bottom-up method of organic nanoelectronics. These fundamental self-assemblies may also find applications as optical elements, memory elements, electrooptic cells, actuators, sensors, etc. The design and synthesis of molecules and the availability of noncovalent interaction mechanisms in solution make it possible to tune the molecular structure to meet the technical requirements for fabrication of efficient devices.

Aromatic molecules have been known for the formation of one-dimentional (1D) nanostructures through strong $\pi-\pi$ interactions.[2–13] These aromatic molecules include porphyrins,[2] hexabenzocoronene derivatives,[3] hexathiapentacene,[4] triphenylenes,[5] phthalocyanines,[6] oligoacenes,[7] perylene tetracarboxylic diimide derivatives,[8–12] etc. Most of the organic materials and their self-assembled nanostructures are of p-type semiconductors.[13] Self-assembly of n-type materials or nanostructures is more demanding in creating p−n junctions or ordered networks with p-type semiconductors for optoelectronic devices, such as solar cells.

Perylene tetracarboxylic diimide derivatives are of interest because of its n-type characteristics.[8] Self-assembly of perylene tetracarboxylic diimide derivatives in solution forms nanostructures including nanobelts,[8,9] nanotubes,[10,11] and nanofibers.[12] Most of these perylene tetracarboxylic diimde derivatives are symmetrical, and the nanostructural morphology was affected by the side chains.[8–12] It is expected that when the two side chains have different hydrophobicities/hydrophilicities, the nanostructural morphology may also be controlled by solvents, depending on the polarity of the solvents. In this work, we report the synthesis and characteristics of a new unsymmetrical, amphiphilic perylene diimide derivative. The compound has self-assembled stacking behavior in both polar and nonpolar solvents. We show that this amphiphilic molecule self-assembled into molecular nanofibers in polar solutions and into nanostrips with well-defined external geometry in nonpolar solutions.

* Corresponding author. E-mail: hji@chem.latech.edu.

## Experimental Section

**I. Materials.** Perylene-3,4,9,10-tetracarboxylic acid dianhydride and decylamine (95%) were purchased from Aldrich (Milwaukee, WI) and used without further purification. Ethoxyethoxyethoxypropylamine was obtained from ChemService (West Chester, PA).

**II. Instruments.** UV−vis spectra were recorded by use of a Shimadzu UV-2401PC spectrophotometer, with temperature control (CPS-Controller) and UV-2401PC software. Fluorescence spectra were obtained using a Hitachi F-2500 fluorescence spectrometer. Proton nuclear magnetic resonance spectra were recorded on a GSX FTNMR spectrometer (JEOL JNM-GSX270 FTNMR). The mass spectra (MS) were obtained with a JEOL AccuTOF-DART system. The temperature for the orifice 1 was set at 80 °C, and the DART temperature was set at 300 °C. The orifice 1 voltage, orifice 2 voltage, and ring lens voltage were 20, 3 and 3, respectively. Helium was used as the DART working gas, and the flow rate was set at 5.6 L/min. The DART needle voltage was 3500 V, and the electrode 1 and 2 voltages were 150 and 250, respectively. A Hitachi FESEM S4800 was used to obtain scanning electron microsopic (SEM) images. A JEOL 2200 FS was used for obtaining transmission electron microscopic (TEM) images.

**III. Synthesis of N-Decylperylene-3,4:9,10-tetracaboxylic-3,4-ethoxyethoxyethoxypropyl-9,10-imide (D1E1).** ***1. Perylene-3,4,9,10-tetracarboxylic Acid Monoanhydride Monopotassium Salt (2).*** Perylene-3,4,9,10-tetracarboxylic acid dianhydride (**1**, 1.96 g, 5 mM) was dissolved in a 5% potassium hydroxide (22.4 g, 20 mM) solution at 90 °C. The resulting solution had a pH of about 10.5. A 14.0 g sample of a 10% acetic acid was added dropwise over 30 min at 90 °C, and the pH was 4.5−5.0. The suspension was stirred for another 1 h at the same temperature; the precipitated bordeaux-colored potassium salt (**2**) was filtered at room temperature, washed with water, and dried at 130 °C. Yield: 2.2 g; 99%. The NMR and MS data were the same as those reported.[14]

10.1021/jp801413k CCC: $40.75 
Published on Web 05/22/2008

**SCHEME 1: Synthetic Route of D1E1**

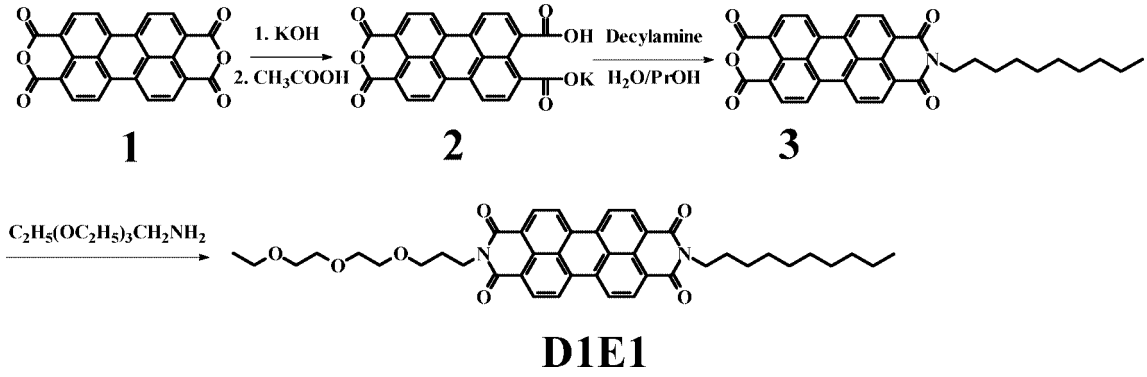


***2. N-Decylperylene-3,4:9,10-tetracarboxylic-3,4-anhydride-9,10-imide (3).*** A mixture of perylene-3,4,9,10-tetracarboxylic acid monoanhydride monopotassium salt **2** (1.25 g, 2.79 mM) and a 4.4 molar ratio of decylamine (1.93 g, 12.3 mM) and 12 mL of $H_2O-PrOH$ (v/v) = 1:1 mixture as solvent was stirred at room temperature for 4 h and heated at 90 °C for 2 h with stirring. The reaction mixture was acidified with 10% hydrochloric acid, and the resulting precipitate was filtered and washed with water to remove residual amine. The residue was stirred into hot 10% potassium hydroxide, and to the mixture was added 8% potassium chloride to separate the precipitated potassium salt of **3** and the symmetrically substituted diimide from the soluble, unreacted **2**. The solid was stirred into water and the insoluble, symmetrically substituted diimide was removed. The filtrate was acidified with 20% hydrochloric acid. The precipitate was filtered, washed with water, and dried to yield **3** in 70.4% yield. The NMR and MS data were the same as those reported.[15]

***3. N-Decylperylene-3,4:9,10-tetracarboxylic-3,4-ethoxyethoxyethoxypropyl-9,10-imide (D1E1).*** *N*-Decylperylene-3,4:9,10-tetracarboxylic-3,4-diacylchloride-9,10-imide (**3**, 0.50 g) and a 1.1 molar ratio of ethoxyethoxyethoxypropylamine and 2 g of 1*H*-imidazole were allowed to react for 4 h at 160 °C under Ar. After cooling of this mixture, 5 mL of water and 80 mL of ethanol were added, and it stood for at least 4 h. The precipitated solid was collected by suction using a glass frit and washed with ethanol. The product was eluted from silica gel column using 1:1:3 $CH_2Cl_2$:hexane:ether mixture. The product was further recrystallized from MeOH. Yield 50%. The compound D1E1 was identified by MS and NMR. MS (*m*/*z*): $C_{43}H_{48}N_2O_7$, 704.35 ($M^+$, 10.21%), 705.35 [$(M + 1)^+$, 100%], 706.35 [$(M + 2)^+$, 45.71%], 727.64 ($M^+ + Na^+$), 743.65 ($M^+ + K^+$). $^1H$ NMR ($CDCl_3$): 8.60−8.69 (q, 8H, perylene), 4.31 (t, 2H, N-$CH_2$), 4.20 (t, 2H, N-$CH_2$), 3.46−3.63 (m, 12H, O-$CH_2$), 2.07−0.85 (m, 24H, $CH_2$, $CH_3$).

## Results and Discussion

Scheme 1 shows the synthetic route of the unsymmetrically substituted biamphiphilic perylene diimide derivative, D1E1. D1E1 contains a hydrophobic long chain at one end and a hydrophilic ethoxy chain at the other. The reaction of perylene dianhydride **1** with primary amine did not produce perylene monoamide **3** directly since the anhydride **1** was either completely converted to diamide **3** or remains unreacted.[16] Simultaneous condensation of **2** with a mixture of two primary amines resulted in a mixture of diimides, including product D1E1, that are difficult to separate. The compound D1E1 was synthesized according to a method introduced by Tröster[17] with modifications. The anhydride **1** was first converted to the tetrapotassium salt, which is readily soluble in water. The monoanhydride monopotassium salt **2** was precipitated by acidification from acetic acid. Owning to the high lattice energy, **3** precipitates from solution and can be removed by filtration.[18] **3** was then condensed to D1E1 with the selected primary amine. The biamphiphilic, unsymmetrical perylene diamide can be such prepared in large scale. All compounds were characterized by $^1H$ NMR spectroscopy and mass spectrometry.

**I. Optical Properties in Solutions.** D1E1 has a fairly high solubility in toluene, THF, and methylene chloride, but precipitates at low concentrations from nonpolar solvents such as

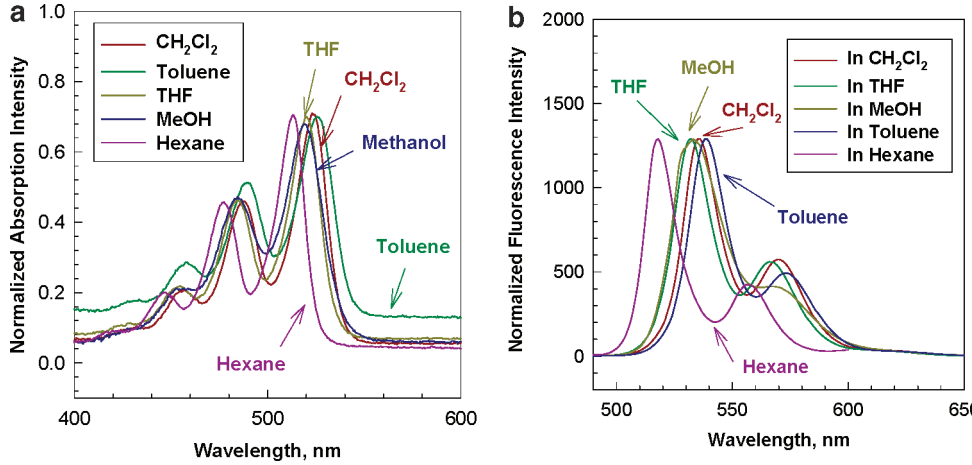


**Figure 1.** UV−vis and fluorescence spectra of D1E1 at 20 °C in hexane, toluene, $CH_2Cl_2$, MeOH, and THF ($1 \times 10^{-6}$ M). Both the absorption and fluorescence spectra were normalized at the 0−0 transition maximum.

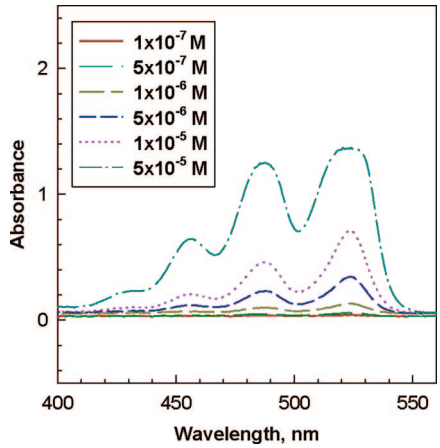


**Figure 2.** UV−vis of D1E1 at 20 °C in $CH_2Cl_2$ at various concentrations.

hexane and methylclohexane, and polar solvents such as methanol and ethanol. The UV−vis and fluorescence spectra of D1E1 in different solvents at low concentration, under which the stacking behavior does not occur or only the clear solutions were used, are shown in Figure 1. In both UV and fluorescence spectra, D1E1 shows a red shift in $CH_2Cl_2$ and toluene solutions, and a blue shift in hexane solution because of different energy levels of the excited states of the perylene moieties. These can be readily explained that in nonpolar solvents such as methylcyclohexane the excited state of the perylene moiety has a relative higher energy than that in polar solvents, and in toluene, the excited state of the perylene moiety can be stabilized by forming a weak peryelne/toluene complex.

The UV−vis spectra of D1E1 in $CH_2Cl_2$ did not show changes in optical properties, except for intensity, on concentration variation between $10^{-7}$ and $5 \times 10^{-5}$ M (Figure 2). Similar UV−vis spectra were observed for D1E1 in THF and toluene. Also, the UV−vis spectra of D1E1 in these solvents did not change at temperature between 20 and 70 °C.

Temperature-dependent UV−vis spectra (Figure 3) of D1E1 showed formation of displaced core J-type aggregate[19] in methanol and face-to-face H-type aggregate[20] in methylcyclohexane. A peak at approximately 570 nm in both solvents suggested the aggregation. In methanol, the stacked form or aggregates appeared when the temperature was lower than 50 °C and the aggregate and monomer forms were reversible under various temperatures. On cooling, the 570 nm peak increased, while the monomer peaks at 450, 478, and 513 nm decreased. These monomer peaks correspond to 0−0, 0−1, and 0−2 electronic transitions, respectively. On heating, the disappearance of the aggregation peak when the temperature was above 50 °C informed the dissolution of the aggregates at higher temperature. In methylcyclohexane, the UV spectrum was clearly indicative of an H-type aggregate since the peak

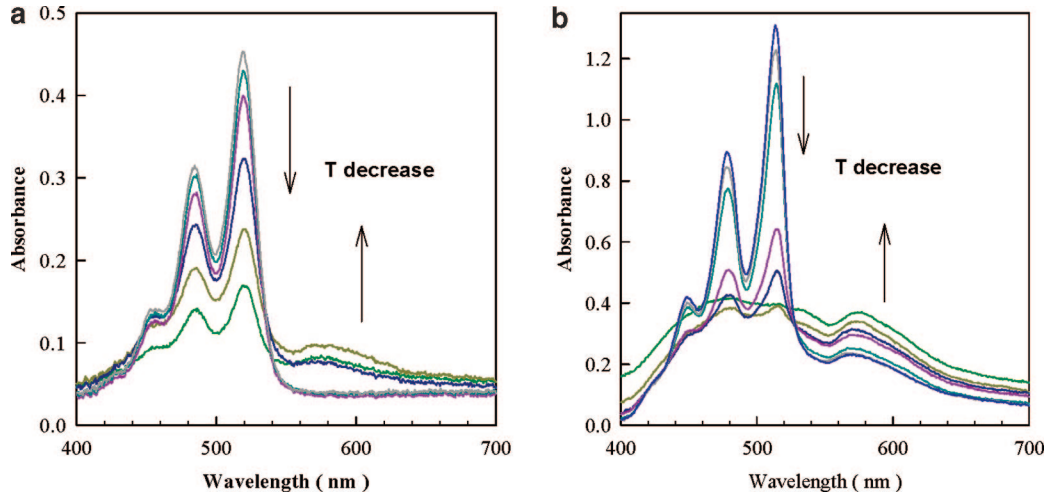


**Figure 3.** Temperature-dependent UV−vis adsorption spectra of D1E1 ($1 \times 10^{-5}$ M) in (a) methanol and (b) methylcyclohexane. Temperature between 20 and 70 °C in 10 °C increments.

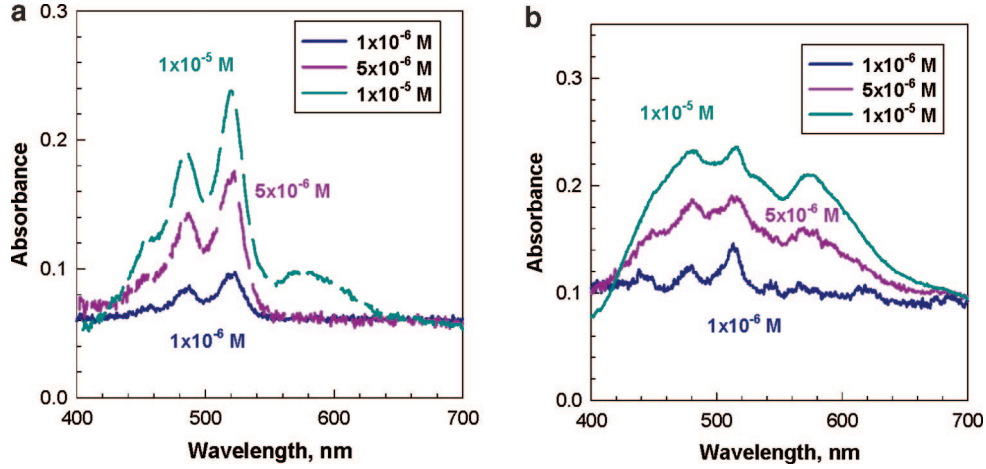


**Figure 4.** Concentration-dependent UV−vis adsorption spectra of D1E1 in (a) methanol and (b) methylcyclohexane.

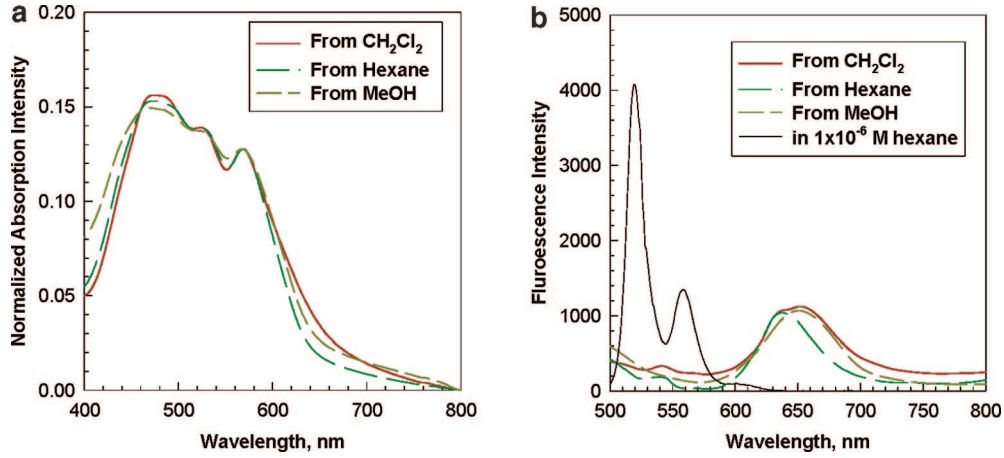


**Figure 5.** UV−vis and fluorescence spectra of D1E1 solids precipitated from MeOH and hexane, and D1E1 solid sample prepared from evaporation of a drop of D1E1 solution in $CH_2Cl_2$ on a quartz substrate. The excitation wavelength was 420 nm.

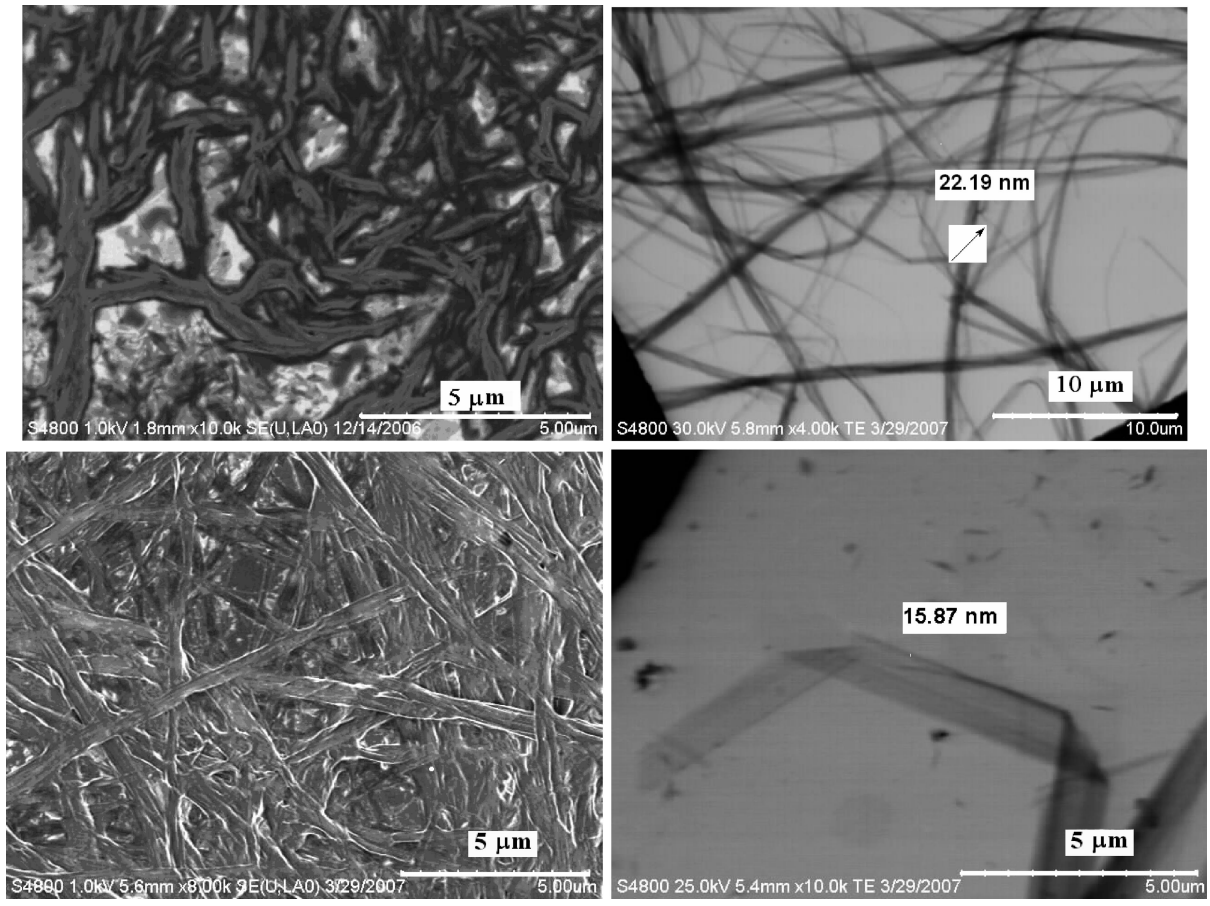


**Figure 6.** SEM images of D1E1 solid prepared from evaporation of a drop of D1E1 solution in $CH_2Cl_2$ on a quartz plate (a, top left), D1E1 solids precipitated from $5 \times 10^{-5}$ M MeOH (b, top right), D1E1 solids precipitated from $1 \times 10^{-3}$ M MeOH (c, bottom left), and D1E1 solids precipitated from $1 \times 10^{-5}$ M hexane (d, bottom right).

corresponding to the aggregation remained upon heating to 70 °C and there was a significant change in the ratio of the intensities of the 0−0/0−1 peaks under various temperatures, which is typical of H-type aggregation.[20] At 20 °C, the UV−vis spectrum of D1E1 in methylcyclohexane was broad and the vibronic fine structures were lost. No red or blue shift of the monomer absorption peaks was an indication of parallel center-to-center transition dipole moments of two perylene moieties in the H-type aggregates.[21]

Concentration-dependent UV−vis measurements (from $1 \times 10^{-6}$ to $1 \times 10^{-5}$ M) also showed the transition from monomeric species to J-type and H-type aggregates of D1E1 in methanol and hexane, respectively (Figure 4). At high concentrations stacks formed in both methanol and methylcyclohexane, whereas at low concentrations the spectra were similar to those in chloroform where no stacking takes place. The ratio of the intensities of 0−0/0−1 peaks did not change in methanol, but did change in methylcyclohexane. D1E1 precipitated from these solvents when the concentration was higher than $5 \times 10^{-5}$ M.

**II. Optical Properties in the Solid State.** D1E1 precipitated from the solution when the concentrations were greater than $1 \times 10^{-5}$ and $5 \times 10^{-5}$ M in methylcyclohexane and methanol,

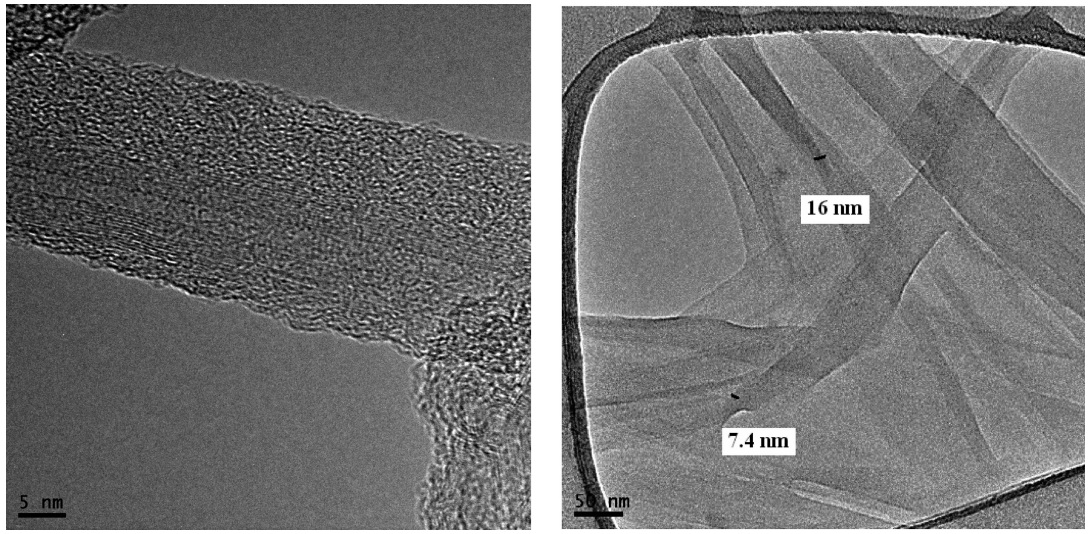


**Figure 7.** TEM images of D1E1 solid precipitated from $5 \times 10^{-5}$ M MeOH (left) and from $1 \times 10^{-5}$ M hexane (right).

**SCHEME 2: Schematic Illustration for the Cross Section of a Bilayered, Nanotubular Structure of D1E1 Aggregates (left) from Methanol and a Double Bilayer Membrane of D1E1 (right) from Methylcyclohexane**

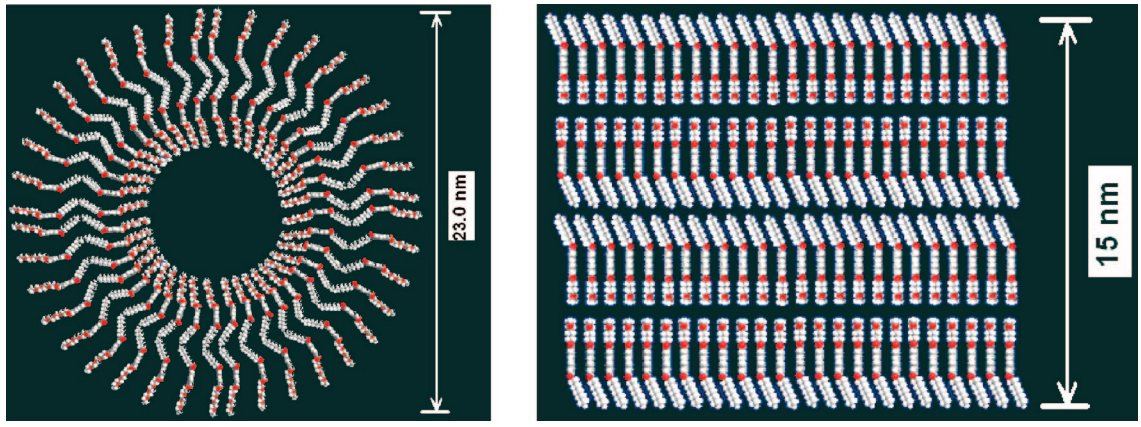


respectively. The aggregation behavior of D1E1 in the solid state was studied by UV spectroscopy, fluorescence spectroscopy, and scanning electron microscopy (SEM). The solids that precipitated from hexane and methanol were transferred to a quartz substrate for analysis. For comparison, another solid sample was prepared from the evaporation of a drop of D1E1 solution in $CH_2Cl_2$ on a quartz substrate. The UV spectra (Figure 5a) of these solids were quite similar to that obtained from hexane solution at higher concentrations, indicating the H-type aggregation of D1E1 in the solid state, which were independent of the solvent. These results showed that at relatively low concentration in methanol the molecule formed J-type aggregates, whereas in the solid state the aggregation changed to H type. Figure 5 shows the fluorescence spectra of the solid samples in comparison with that in $1 \times 10^{-6}$ M hexane. All the fluorescence spectra in the solid state showed a new emission

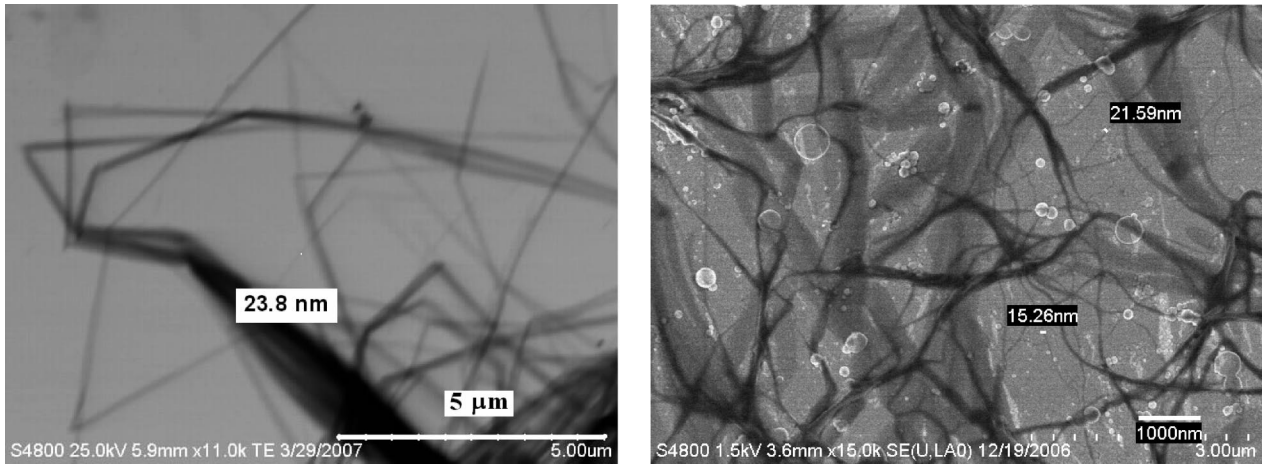


**Figure 8.** SEM images of D1E1 nanofibers precipitated from THF ($1 \times 10^{-4}$ M, left) and THF−water (1:1) mixture ($1 \times 10^{-6}$ M, right).

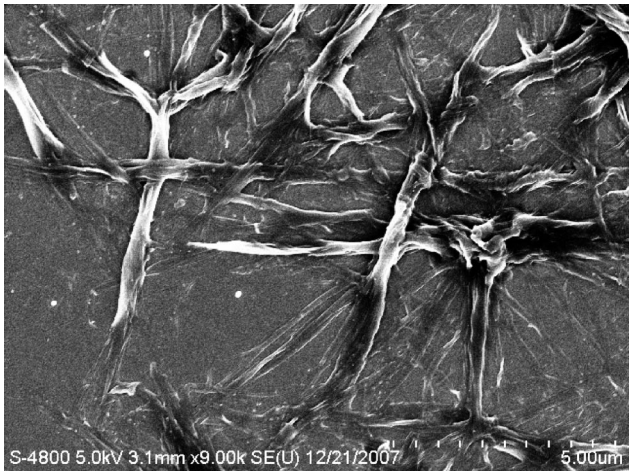


**Figure 9.** SEM images of D1E1 solid precipitated from $1 \times 10^{-5}$ M 1:1 MeOH/methylcyclohexane mixture.

band at approximately 640 nm, which corresponds to the emission from the aggregates (Figure 5b). The monomer peaks were all gone, suggesting strong $\pi-\pi$ stacking and a typical H-type aggregation behavior.[22]

The SEM images (Figure 6) showed the aggregation variations of the three solid samples. The solid from the evaporation of $CH_2Cl_2$ on the substrate showed a self-assembled network structure (Figure 6a), which was less ordered than the solids precipitated from hexane and methanol. The solid precipitated from methanol was in the form of nanofibers hundreds of micrometers long. The narrowest fibers precipitated from $5 \times 10^{-5}$ M in methanol were approximately 22 nm (Figure 6b). The bolder fibers were composed of a bundle of narrow nanofibers. The diameters of the nanofiber bundles increased when D1E1 was precipitated from higher concentrations of methanol ($5 \times 10^{-5}-1 \times 10^{-4}$ M), and the bundles became a tangled network structure when D1E1 was precipitated from even higher concentrations ($1 \times 10^{-4}-1 \times 10^{-3}$ M) of methanol (Figure 6c). The solids that precipitated from nonpolar solvents, such as hexane and methylcyclohexane, however, showed a nanostrip structure, approximately 500 nm in width and approximately 16 nm in thickness (Figure 6d). The nanostrips from hexane were relatively shorter than those nanofibers prepared from methanol. It is noteworthy that the dimensional value shown in SEM was not precise because of the resolution. A transmission electron microscopy (TEM) image of the nanofiber (Figure 7, left), however, showed that the diameter of the finest nanofiber was $21.83 \pm 1.17$ nm. The identification of the nanostrip edge from the TEM image of the solid precipitated from hexane was not apparent as was that of the nanofibers, but it is possible that nanostrips of both 7.4- and 16-nm thickness exist as shown from Figure 7, right.

Based on the optical properties in the solid state and the nanostructure dimensions, the molecular structures of these nanoassemblies precipitated from methanol and methylcyclohexane are proposed in Scheme 2. In methanol, the nanofiber structure was similar to a typical rod-like micelle in water. Considering the dimensions of the nanofiber measured from SEM and TEM images and the spectra, it is most likely that the D1E1 nanofibers from methanol were made of a bilayer of D1E1 molecules; i.e., the hydrophilic ethoxy chains were both inside and outside the nanotubular structure exposed to the polar solvent and the hydrophobic alkyl groups were in the middle of the bilayer tubing. In methylcyclohexane, the SEM image showed the film-like nanostrips which would be made of a bilayer membrane of D1E1 molecules and the hydrophobic alkyl chains were exposed to nonpolar solvents outside. Although a bilayer membrane of D1E1 is possible, the thickness of the membrane showed that it is possible both single and double bilayers of the membrane exist. The scheme of a double bilayer is shown in Scheme 2, right.

Similar nanofiber and nanostrip structures were observed on precipitates from ethanol and hexane, respectively. The solids precipitated from other polar solvents, such as THF at high concentration and THF/$H_2O$ 1:1 mixture (Figure 8), were also in the form of a nanofiber structure as those from alcohol due to the amphiphilic structure. The dimensions of the narrowest nanofibers were close to that from methanol. The solids precipitated from methanol/methylcyclohexane, however, showed a less ordered self-assembled network structure (Figure 9).

The drain characteristics of the nanofibers (Figure 10) showed n-type semiconductivity. The applied gate-source voltage, $V_{GS}$, changed the current between the source and the drain ($I_D$). It is noteworthy that the conductivity of a single nanofiber was too weak to be measured, and the drain characteristics of D1E1 nanofibers in Figure 10 were measured on a bunch of nanofibers between the source and the drain.

The aggregation behaviors of perylene diimides with two symmetrical alkyl[9] or alkoxy[8] units have been previously

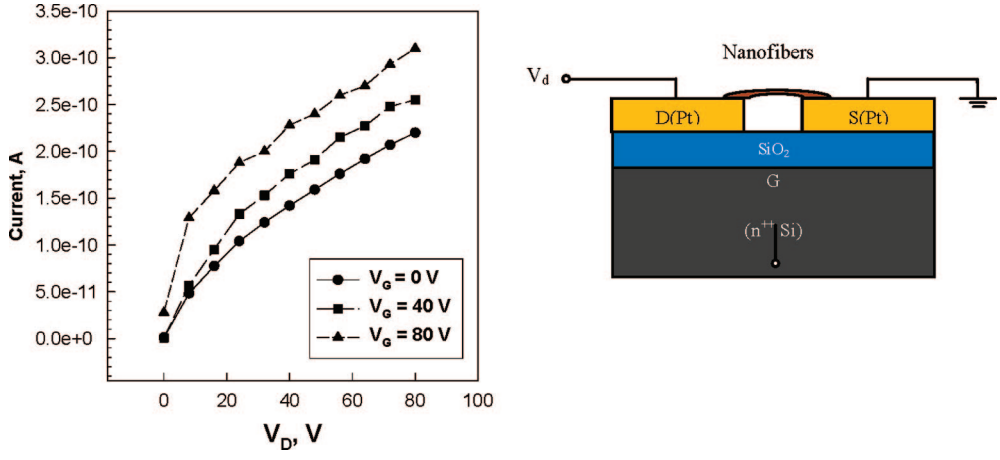


**Figure 10.** *I*−*V* curve of D1E1 nanofibers. The nanofibers were drop-cast on a silicon substrate between two gold electrodes. Heavily doped n-type Si with resistivity <0.005 Ω was used as the gate electrode. Platinum (Pt) patterned by means of lift-off photolithography was used as the source and drain electrodes. $SiO_2$ (300 nm) was used as the gate dielectric.

reported. Those molecules form nanobelts in both polar and nonpolar solvents, and the solvents do not affect the morphology of the nanoassembly. Our work focused the line of studies aimed at building artificial heterogeneous molecular systems controlled by solvent. In summary, we showed supramolecular stacks of an unsymmetrical, amphiphilic perylene diimide, D1E1, obtained in both polar and nonpolar solutions. Our study suggested that, by varying the hydrophobicity of the side groups, two types of self-assembled nanostructures can be obtained from polar and nonpolar solvents.

**Acknowledgment.** This work was supported by NSF Sensor and Sensor Network ECS-0428263. Dr. Zhanpin Wu from JEOL is acknowledged for the mass spectrometry experiments. Drs. Sheng Dai and Karren More are acknowledged for the TEM images.

**Supporting Information Available:** NMR and MS results and additional figures. This material is available free of charge via the Internet at http://pubs.acs.org.

## References and Notes

(1) Green, J. E.; Choi, J. W.; Boukai, A.; Bunimovich, Y.; Johnston-Halperin, E.; Delonno, E.; Luo, Y.; Sheriff, B. A.; Xu, K.; Shin, Y. S.; Tseng, H.-R.; Stoddart, J. F.; Health, J. R. *Nature,* **2007**, *445*, 414–417.

(2) Duzhko, V.; Singer, K. D. *J. Phys. Chem. C* **2007**, *111*, 27–31.

(3) Hill, J. P.; Jin, W.; Kosaka, A.; Fukushima, T.; Ichihara, H.; Shimomura, T.; Ito, K.; Hashizume, T.; Ishii, N.; Aida, T. *Science* **2004**, *304*, 1481–1483.

(4) Briseno, A. L.; Mannsfeld, S. C. B.; Lu, X.; Xiong, Y.; Jenekhe, S. A.; Bao, Z.; Xia, Y. *Nano Lett.* **2007**, *7*, 668–675.

(5) Glusen, K.; Singer, D.; Kohne, B.; Ebert, M.; Liebmann, A.; Wendorff, J. H. *Liq. Cryst.* **1991**, *10*, 147–159.

(6) Tang, Q.; Li, H.; He, M.; Hu, W.; Liu, C.; Chen, K.; Wang, C.; Liu, Y.; Zhu, D. *Adv. Mater.* **2006**, *18*, 65–68.

(7) Bendikov, M.; Wudl, F.; Perepichka, D. F. *Chem. Rev.* **2004**, *104*, 4891–4945.

(8) Balakrishnan, K.; Datar, A.; Oitker, R.; Chen, H.; Zuo, J.; Zang, L. *J. Am. Chem. Soc.* **2005**, *127*, 10496–10497.

(9) Balakrishnan, K.; Datar, A.; Naddo, T.; Huang, J.; Otiker, R.; Yen, M.; Zhao, J.; Zang, L. *J. Am. Chem. Soc.* **2006**, *128*, 7390–7398.

(10) Sinks, L. E.; Rybtchinski, B.; Iimura, M.; Jones, B. A.; Goshe, A. J.; Zuo, X.; Tiede, D. M.; Li, X.; Wasielewski, M. R. *Chem. Mater.* **2005**, *17*, 6295–6303.

(11) Gesquiere, A.; Jonkheijm, P.; Hoeben, F. J. M.; Schenning, A. P. H. J.; De Feyter, S.; De Schryver, F. C.; Meijer, E. W. *Nano Lett.* **2004**, *4*, 1175–1179.

(12) Schenning, A. P. H.; Herrikhuyzen, J. V.; Jonkheijm, P.; Chen, Z.; Wurthner, F.; Meijer, E. W. *J. Am. Chem. Soc.* **2002**, *124*, 10252–10253.

(13) Xu, B. Q.; Xiao, X.; Yang, X.; Zang, L.; Tao, N. J. *J. Am. Chem. Soc.* **2005**, *127*, 2386–2387.

(14) Tröster, H. *Dyes Pigm.* **1983**, *4*, 171.

(15) Nagao, Y.; Naito, T.; Abe, Y.; Misono, T. *Dyes Pigm.* **1996**, *32*, 71–83.

(16) Herrikhuyzen, J. V.; Syamakumari, A.; Schenning, A. P. H.; Meijer, E. W. *J. Am. Chem. Soc.* **2004**, *126*, 10021–10027.

(17) Tröster, H. *Dyes Pigm.* **1983**, *4*, 171–177.

(18) Nagao, Y.; Naito, T.; Abe, Y.; Misono, T. *Dyes Pigm.* **1996**, *32*, 71–83.

(19) Herrikhuyzen, J. V.; Syamakumari, A.; Schenning, A. P. H.; Meijer, E. W. *J. Am. Chem. Soc.* **2004**, *126*, 10021–10027.

(20) Jancy, B.; Asha, S. K. *Chem. Mater.* **2008**, *20*, 169–181.

(21) Beckers, E. H.; Chen, Z.; Meskers, S. C. J.; Jonkheijm, P.; Schenning, A. P. H. J.; Li, X. Q.; Osswald, P.; Wurthner, F.; Janssen, R. A. J. *J. Phys. Chem. B* **2006**, *110*, 16767–16978.

(22) Wurthner, F.; Chen, Z.; Dehm, V.; Stepanenko, V. *Chem. Commun.* **2006**, 1188–1190.

JP801413K